

---

This is an electronic reprint of the original article.  
This reprint may differ from the original in pagination and typographic detail.

Mirmoosa, Mohammad S.; Kosulnikov, Sergei; Simovski, Constantin R.  
**Unbounded spatial spectrum of propagating waves in a polaritonic wire medium**

*Published in:*  
Physical Review B

*DOI:*  
[10.1103/PhysRevB.92.075139](https://doi.org/10.1103/PhysRevB.92.075139)

Published: 01/01/2015

*Document Version*  
Publisher's PDF, also known as Version of record

*Please cite the original version:*  
Mirmoosa, M. S., Kosulnikov, S., & Simovski, C. R. (2015). Unbounded spatial spectrum of propagating waves in a polaritonic wire medium. *Physical Review B*, 92(7), 1-7. Article 075139.  
<https://doi.org/10.1103/PhysRevB.92.075139>

---

This material is protected by copyright and other intellectual property rights, and duplication or sale of all or part of any of the repository collections is not permitted, except that material may be duplicated by you for your research use or educational purposes in electronic or print form. You must obtain permission for any other use. Electronic or print copies may not be offered, whether for sale or otherwise to anyone who is not an authorised user.

**Unbounded spatial spectrum of propagating waves in a polaritonic wire medium**M. S. Mirmoosa,<sup>1</sup> S. Yu. Kosulnikov,<sup>1,2</sup> and C. R. Simovski<sup>1,2</sup><sup>1</sup>*Department of Radio Science and Engineering, School of Electrical Engineering, Aalto University, P.O. Box 13000, FI-00076 AALTO, Finland*<sup>2</sup>*Department of Nanophotonics and Metamaterials, ITMO University, 197043 St. Petersburg, Russia*

(Received 24 April 2015; revised manuscript received 29 July 2015; published 26 August 2015)

In this paper, we study a topological phase transition in a wire medium operating at infrared frequencies. This transition occurs in the reciprocal space between the indefinite (open-surface) regime of the metamaterial and its dielectric (closed-surface) regime. Due to the spatial dispersion inherent to a wire medium, a hybrid regime turns out to be possible at the transition frequency. Both such surfaces exist at the same frequency and touch one another. At this frequency, all values of the parallel wave vector correspond to propagating spatial harmonics. The implication of this regime is the overwhelming radiation enhancement. We numerically investigate the gain in radiated power for a subwavelength dipole source submerged into such medium. In contrast to previous works, this gain (called the Purcell factor) turns out to be higher for a parallel dipole than for a perpendicular one.

DOI: [10.1103/PhysRevB.92.075139](https://doi.org/10.1103/PhysRevB.92.075139)

PACS number(s): 41.20.Jb, 81.05.Xj, 78.67.Uh, 74.25.Gz

**I. INTRODUCTION**

Electromagnetic metamaterials are artificial media structured on the subwavelength level which exhibit extraordinary electromagnetic features and functionalities that are not found in nature. The most popular examples of these unusual functionalities can be the negative refractive index [1], transformation optics [2], and perfect lens [3].

Many metamaterials possess unusual dispersion properties. For regular metamaterials (lattices), their dispersion properties are described in terms of dispersion surfaces, also called Fresnel's wave or isofrequency surfaces. A dispersion surface defines wave vectors for all propagation directions at the given frequency in the reciprocal space of the lattice. One striking example of metamaterials is hyperbolic ones, so called because their dispersion surface is hyperboloid. Such metamaterials are exploited in a variety of applications, including subwavelength imaging [4], radiative heat transfer [5,6], and enhancement of radiation (called the Purcell factor [7]) for emitters embedded into such media [8–10]. Indeed, a nonmagnetic hyperbolic metamaterial is most popular in optics, where magnetic properties are very difficult to realize. Optical hyperbolic metamaterials are anisotropic media whose principal components (more exactly, real parts) of the effective permittivity tensor have different signs. Because of the indefinite sign of the permittivity tensor trace, such media are also called indefinite [11]. The most expanded are the indefinite (hyperbolic) media of uniaxial type. The different signs of two principal components of the permittivity tensor imply the hyperboloid of revolution in the reciprocal space.

Uniaxial hyperbolic metamaterials operating in the optical range are usually implemented as a stack of bilayers. One layer of the unit cell is a material with negative dielectric response and the other layer is a transparent material. Another known implementation of hyperbolic metamaterial is a regular optically dense array of parallel wires called a wire medium (see, e.g., Refs. [8,12]). The homogenization models known for both kinds of hyperbolic metamaterials (see Refs. [8,12–14]) point to the possibility of a sharp qualitative change of their dispersion regime versus frequency. When the frequency varies, one of two principal components of the permittivity tensor may

keep its sign whereas the sign of the other component changes. Then the hyperboloid (open surface) in the reciprocal space transforms into a closed surface, e.g., an ellipsoid. This transition is similar to the known Lifshitz topological transitions in metals [15] (when the Fermi surfaces change their topology similarly). Therefore, this jump of the dispersion properties was entitled “topological phase transition” in Ref. [16]. One interesting problem is the topological transition happening in the reciprocal space. To have such an exotic phenomenon, the open and closed surfaces should be connected to each other in the reciprocal space. The coexistence of open and closed surfaces has been observed in photonic crystal media [17] which are not subwavelength structures. For typical hyperbolic metamaterials, the coexistence of these two surfaces is due to the different propagating modes (ordinary and extraordinary) in the medium [18]. The open surface corresponds to the extraordinary mode and the closed surface corresponds to the ordinary mode. However, in Ref. [19], a metamaterial has been suggested with both surfaces for one mode. In this paper, we show that in a wire medium of polaritonic rods operating at midinfrared, it is also possible to have the coexistence of the proposed surfaces at the same frequency only for the extraordinary mode. Most importantly, the surfaces touch one another at two specific points in the reciprocal space. The phenomenon arises from the nonlocal response of the wire medium and this kind of topological phase transition is different from that studied in Refs. [16,20,21]. It provides an unbounded spatial spectrum which should cause a high Purcell factor due to the absence of any cutoff for spatial harmonics. Hence, we validate our finding via the exact calculation of the Purcell factor. We show how a huge Purcell factor is achieved for a subwavelength electric dipole oriented in parallel to the optical axis of the medium. This result diverges from the previously known results. The Purcell factor of “standard” (purely hyperbolic) wire media attains two orders of magnitude for a dipole oriented perpendicular to the optical axis, whereas for a parallel dipole, it is much smaller [8,10,22,23]. Here, we show that in the transition regime, the Purcell factor of a perpendicular dipole stays nearly the same as in the hyperbolic regime, while for a parallel dipole, it exceeds two orders of magnitude.

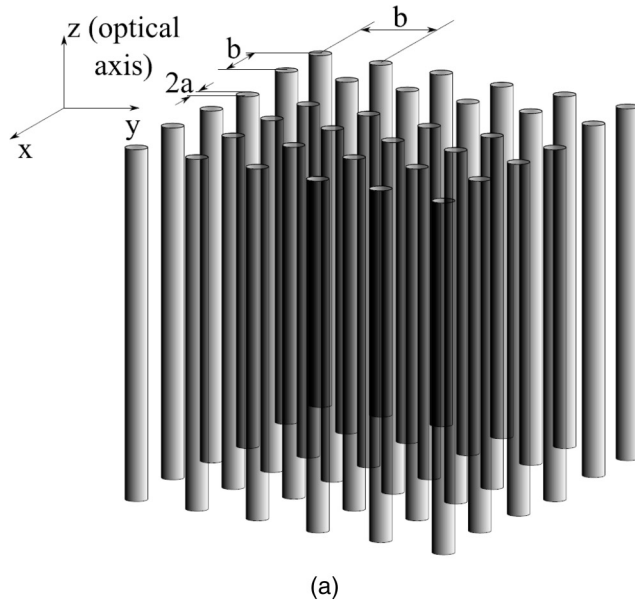
Our paper is organized as follows: in Sec. II, we introduce the approach used to achieve the unbounded spatial spectrum in a wire medium. Section III presents the numerical results for the Purcell factor and gives some discussion of their interpretation. Finally, Sec. IV concludes the paper.

## II. THEORY

The electromagnetic properties of a general wire medium, shown in Fig. 1(a), are described through a homogeneous effective permittivity tensor as

$$\bar{\bar{\epsilon}} = \begin{pmatrix} \epsilon_{xx} & 0 & 0 \\ 0 & \epsilon_{yy} & 0 \\ 0 & 0 & \epsilon_{zz} \end{pmatrix} = \begin{pmatrix} \epsilon_{\perp} & 0 & 0 \\ 0 & \epsilon_{\perp} & 0 \\ 0 & 0 & \epsilon_{\parallel} \end{pmatrix}. \quad (1)$$

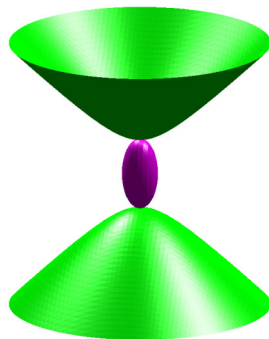
As Fig. 1(a) illustrates,  $\mathbf{z}_0$  is the optical axis of the medium that coincides with the wire axis. In the case of thin and negative-dielectric constant wires, the perpendicular ( $\epsilon_{\perp}$ ) and parallel ( $\epsilon_{\parallel}$ ) components of the effective tensor are given



(a)



(b)



(c)

FIG. 1. (Color online) (a) Long parallel wires which are set in a square lattice. The host material is air. (b) Isofrequency surface of ordinary mode. (c) Topological phase transition for the extraordinary mode giving unbounded spatial spectrum. The typical type-I hyperbolic dispersion (green surface) coexists with a connected ellipsoidal dispersion (purple surface).

by [14]

$$\epsilon_{\perp} = \epsilon_h + \frac{2\epsilon_h}{\frac{\epsilon_r + \epsilon_h}{f_v(\epsilon_r - \epsilon_h)} - 1}, \quad (2)$$

$$\epsilon_{\parallel} = \epsilon_h + \frac{\epsilon_h}{\frac{\epsilon_h}{f_v(\epsilon_r - \epsilon_h)} - \frac{k_h^2 - \beta^2}{k_p^2}}.$$

Here,  $\epsilon_h$  and  $\epsilon_r$  are the permittivity of the host medium and the wires, respectively, and  $f_v$  denotes the volume fraction. In this paper, we assume that the host medium is air, i.e.,  $\epsilon_h = 1$ . In addition,  $k_h = k_0$  is the free-space wave number,  $\beta$  is the parallel component of the wave vector in the wire medium, and  $k_p$  is called the plasma wave number:

$$k_p = \frac{1}{b} \sqrt{\frac{2\pi}{0.5275 + \ln\left(\frac{b}{2\pi a}\right)}}. \quad (3)$$

Since the wire medium is a uniaxial, two modes exist in it. The first mode is the ordinary transverse-electric (TE) wave and the second one is the extraordinary transverse-magnetic (TM) wave. Solving Maxwell's equations, the dispersion relation of ordinary and extraordinary waves can be expressed as [24]

$$q^2 + \beta^2 = k_0^2 \epsilon_{\perp}, \quad \text{ordinary (TE) mode} \quad (4)$$

$$\frac{q^2}{\epsilon_{\parallel}(\beta)} + \frac{\beta^2}{\epsilon_{\perp}} = k_0^2, \quad \text{extraordinary (TM) mode,}$$

where  $q$  is the perpendicular component of the wave vector. Here,  $\epsilon_{\parallel}$  is a function of  $\beta$ . Normally, purely local effective medium theories are sufficient for optically dense composites unless the impact of ultralarge lateral wave vectors is strong. This refers also to stacked hyperbolic metamaterials of metal (or, generally, a material with negative dielectric response) and transparent layers [25]. For wire media, the spatial dispersion is linked to nonzero  $\beta$  [14].

For simplicity, let us assume that the wires are lossless. If their volume fraction is small enough and the relative dielectric constant of the wire material is not very close to  $-1$ , the perpendicular component  $\epsilon_{\perp}$  is positive and approximately equals unity (in the general case, to that of the host dielectric material). Based on Eq. (4), the ordinary wave has a closed-surface dispersion, as shown in Fig. 1(b) (a sphere with a radius equal to  $\sqrt{\epsilon_{\perp}} \approx 1$ ), and therefore does not support large wave vectors. We are definitely interested in the extraordinary wave because the hyperbolic dispersion corresponds only to this mode. Equation (4) indicates that if  $\epsilon_{\parallel} < 0$ , a hyperbolic dispersion arises (hyperbolic media of type I; see, e.g., Ref. [26]) that implies propagation of waves with high values of both parallel and perpendicular wave vectors. In this case, the evanescent waves usually produced by a subwavelength dipole source are converted into propagating waves, resulting in the high Purcell factor.

However, in hyperbolic dispersion, as seen from Eq. (4), there is a cutoff for the parallel component of the wave vector:  $\beta \geq k_0 \sqrt{\epsilon_{\perp}}$ . To prominently increase the Purcell factor, we need to eliminate this cutoff. For  $\beta < k_0 \sqrt{\epsilon_{\perp}}$ , based on Eq. (4), the propagation becomes possible if  $\epsilon_{\parallel} > 0$  (elliptical dispersion). We need to unify both the elliptical and hyperbolic

dispersions at the same frequency so that these branches touch each other at the transition point  $\beta = k_0\sqrt{\varepsilon_\perp}$ , as shown in Fig. 1(c). This is possible because the parallel component of permittivity in Eq. (4) depends on the wave vector.

If we substitute Eq. (2) in Eq. (4), the perpendicular wave vector can be expressed as

$$q^2 = \frac{1}{\varepsilon_\perp} [\beta^2 - R_1][\beta^2 - R_2] \frac{f_v(1 - \varepsilon_r)}{k_p^2 - f_v(\varepsilon_r - 1)(k_0^2 - \beta^2)}, \quad (5)$$

where

$$R_1 = \frac{f_v(\varepsilon_r - 1)k_0^2 - (1 + f_v(\varepsilon_r - 1))k_p^2}{f_v(\varepsilon_r - 1)},$$

$$R_2 = k_0^2\varepsilon_\perp. \quad (6)$$

If the roots  $R_1$  and  $R_2$  are equivalent and  $f_v(1 - \varepsilon_r) > 0$ , then the value  $q^2$  is always positive, which results in the propagating mode for any  $\beta$ . The cutoff of the spatial spectrum is removed at this frequency, and we have

$$f_v(1 - \varepsilon_r) = \frac{k_p^2}{k_p^2 + (\varepsilon_\perp - 1)k_0^2}. \quad (7)$$

Since the plasma wave number is very large compared to  $\sqrt{\varepsilon_\perp - 1}k_0$  [ $k_p^2 \gg (\varepsilon_\perp - 1)k_0^2$ ], the needed permittivity of the wire material can be approximated as

$$\varepsilon_r = 1 - \frac{1}{f_v}. \quad (8)$$

The condition expressed in Eqs. (7) and (8) results in  $\varepsilon_\parallel = 0$  at the point  $\beta = k_0\sqrt{\varepsilon_\perp}$  in the isofrequency surface. Based on Eq. (2), it can be easily shown that for  $\beta < k_0\sqrt{\varepsilon_\perp}$ ,  $\varepsilon_\parallel$  is positive (corresponding to nearly elliptical dispersion), and for  $\beta > k_0\sqrt{\varepsilon_\perp}$ ,  $\varepsilon_\parallel$  is smaller than zero (corresponding to nearly hyperbolic dispersion). Figure 1(c) shows the topological phase transition. Since the permittivity tensor depends on the wave vector, we do not obtain exactly hyperboloidal and ellipsoidal parts of the dispersion surface. Therefore, instead of hyperboloid and ellipsoid, we prefer to use more exact terms: open surface and closed surface, respectively.

Figure 2(a) shows the parallel component of the effective permittivity versus the normalized parallel wave vector at the optimized wavelength in which the topological transition happens. In this example, the fraction of wires is  $f_v = 0.05$  that makes the relative dielectric constant of the wire material equal to  $\varepsilon_r = -19$  in according to Eq. (8). The figure has specified the closed-surface (positive-permittivity) and the open-surface (negative-permittivity) regimes. The transition happens at  $\beta b = \pm 1$ , where  $\varepsilon_\parallel(\beta) = 0$ . The corresponding isofrequency curve is shown in Fig. 2(b). Different isofrequency surfaces for several values of relative dielectric constant of the wires are shown in Fig. 3. It is easily seen that the optimal regime corresponds to the blue solid curve representing  $\varepsilon_r = -19$  when there is no spatial-frequency cutoff. When  $\varepsilon_r = -23$ , the closed surface does not exist and the cutoff is present. Gradually reducing the absolute value of the relative dielectric constant causes the positive-permittivity regime to appear. Both parts of the isofrequency surface touch each other at the point  $\varepsilon_\parallel = 0$  if  $\varepsilon_r = -19$ .

So, a topological phase transition in a wire medium whose  $f_v = 0.05$ ,  $\lambda/b = 6.6$  ( $\lambda$  is the free-space wavelength), and

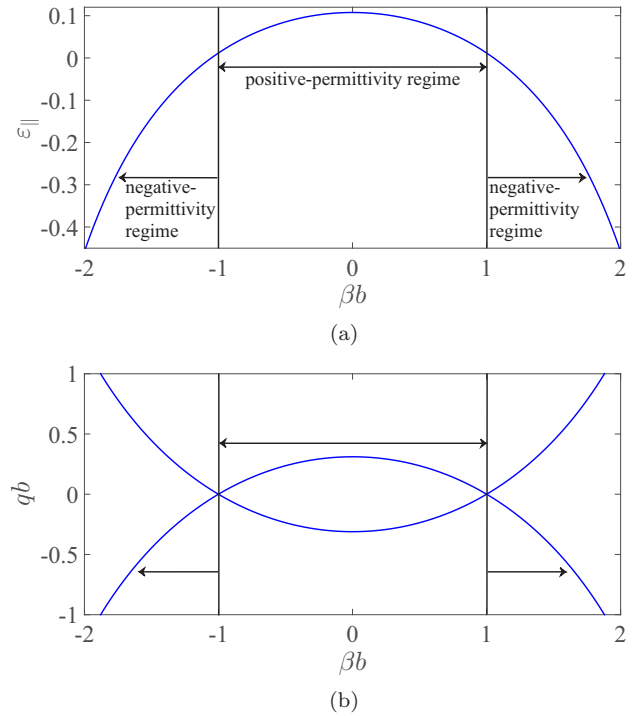


FIG. 2. (Color online) (a) Parallel component of effective permittivity with respect to normalized wave vector and (b) corresponding isofrequency contour (cross section of the dispersion surface) for the extraordinary (TM) mode. Calculations are related to the following values:  $f_v = 0.05$  and  $\lambda/b = 6.6$ , where  $\lambda$  is the free-space wavelength.

wires have relative permittivity close to  $-19$  is possible in the frequency range where the nonlocal homogenization model [14] is applicable. This model has been recognized for its high accuracy [12].

As mentioned already in Sec. I, a topological transition happens not because the effective permittivity changes its sign over the frequency axis as in Refs. [16,20]. In our case, the effective permittivity changes the sign over the wave-vector axis, and both closed-surface and open-surface branches exist in the reciprocal space together and touch one another. Notice that such phenomenon is, in principle, known in the theory of metamaterials with spatial dispersion. In Ref. [19], a spatially dispersive metamaterial for which both hyperboloid and ellipsoid surfaces simultaneously exist in the reciprocal space is suggested and theoretically studied. The suggested metamaterial in Ref. [19] is an ultimately anisotropic strictly regular lattice of uniaxial strongly resonant inclusions. In optics, such an array could be implemented from very thin and substantially long Ag (silver) or Au (gold) nanorods operating at their plasmon resonance. Varying the geometric parameters, one may engineer the regime of unbounded spatial spectrum when the open and closed branches of the dispersion surface would be touching or intersecting.

However, the metamaterial [19] is challenging for practical realization at optical frequencies, and its experimental verification in the near future is problematic. Meanwhile, the spatial dispersion which is needed to unify the elliptical and hyperbolic dispersion branches turns out to be possible in a wire medium. In the next section, we consider an

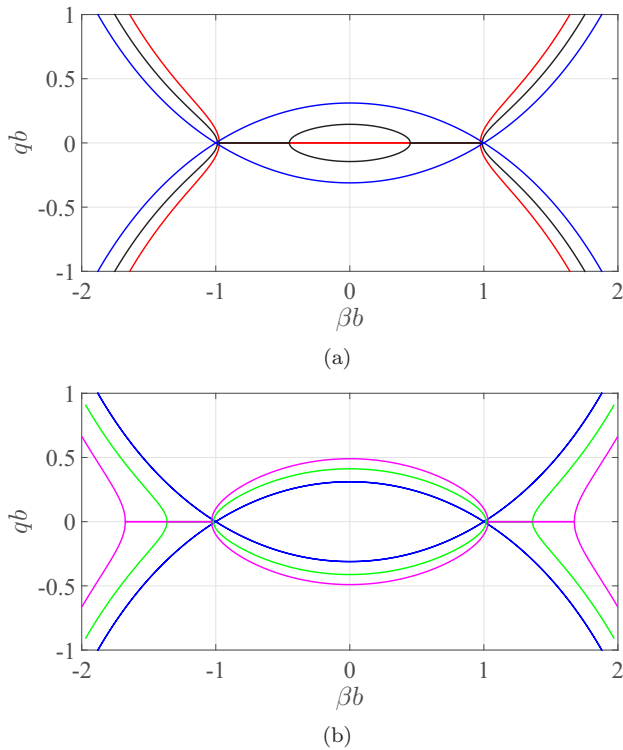


FIG. 3. (Color online) Isofrequency contour (cross section of the dispersion surface) of the extraordinary (TM) mode for different values of the relative dielectric constant of the wires. Calculations are related to the following values:  $f_v = 0.05$  and  $\lambda/b = 6.6$ . The curves based on their colors correspond to  $\epsilon_r = -23$  (red),  $\epsilon_r = -20.75$  (black),  $\epsilon_r = -19$  (blue),  $\epsilon_r = -17$  (green), and  $\epsilon_r = -15.35$  (magenta).

implementation of the wire medium at mid-IR range. At these frequencies, polaritonic materials are suitable for our purpose and, as an example, we focus on lithium tantalate ( $\text{LiTaO}_3$ ). The idea is transferable into other polaritonic materials, e.g., SiC. Aligned nanowires of polaritonic materials grown in a solid matrix have been reported since 2009, when the first paper on them was published [27]. Although the instance of polaritonic wire media with freestanding parts is not known, there are no basic technological limitations, and we hope that it will be reported soon.

### III. RESULTS AND DISCUSSION

The topological phase transition should result in a high Purcell factor since there is no cutoff for spatial harmonics. Therefore, we calculated the Purcell factor in order to confirm our finding. We performed full-wave, three-dimensional (3D) simulations employing the CST Microwave Studio simulator. For reliability, some simulation results were also reproduced using the HFSS software. The sample of wire medium in our simulations is of cubic shape, and the volume fraction is equal to  $f_v = 0.0804$ . This value may correspond, for example, to the wire radius  $a = 32$  nm and period  $b = 200$  nm. Based on Eq. (8), the relative dielectric constant of the wires should have  $\text{Re}(\epsilon_r) = -11.4$  and  $|\text{Im}(\epsilon_r)| \ll |\text{Re}(\epsilon_r)|$  that allows  $\epsilon_{\perp} \approx 0$  at the point  $\beta = k_0\sqrt{\epsilon_{\perp}}$  and, subsequently, the

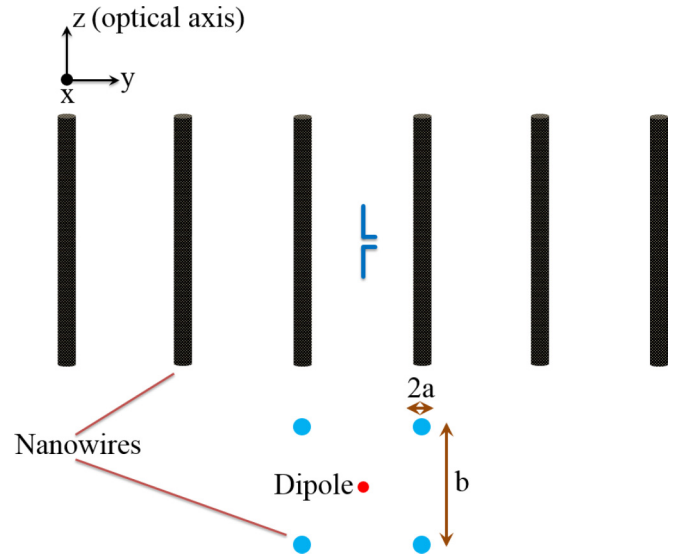


FIG. 4. (Color online) Geometry and orientation of the subwavelength electric dipole source in the metamaterial sample.

transition from the negative-permittivity regime [ $\text{Re}(\epsilon_{\parallel}) < 0$ ] to the positive-permittivity regime [ $\text{Re}(\epsilon_{\parallel}) > 0$ ]. Because  $\text{Re}(\epsilon_r)$  is negative, the transition is, in principle, possible for metal nanowires within the visible range. However, this option requires either very tiny nanowires, which will be challenging for fabrication, or a more sparse array for which the transition occurs at the wavelength beyond the domain of applicability of the homogenization model. Another option is using polaritonic materials, e.g., lithium tantalate operating in the near-IR or mid-IR ranges. Notice that at these frequencies, metals are not suited because the skin depth is too small and the field interacts insufficiently with the metallic rod. The dielectric function of polaritonic materials is provided by the Drude-Lorentz model [28],  $\epsilon_r = \epsilon_{\infty}[1 + (\omega_L^2 - \omega_T^2)/(\omega_T^2 - \omega^2 + j\omega\gamma)]$ , where for  $\text{LiTaO}_3$  we have  $\omega_T/2\pi = 26.7$  THz,  $\omega_L/2\pi = 46.9$  THz,  $\gamma/2\pi = 0.94$  THz, and  $\epsilon_{\infty} = 13.4$  [29,30]. The value  $\epsilon_r = -11.4$  corresponds to the permittivity of lithium tantalate at about  $f = 39$  THz.

The emitter is chosen to be a subwavelength electric dipole. We have studied different orientations and locations of this dipole inside the wire medium sample. Here, we show the results for both longitudinal (dipole parallel to nanowires and optical axis) and perpendicular (dipole perpendicular to optical axis) orientations and compare the results. In both cases, the dipoles are located symmetrically in the gap between nanowires at the center of the wire medium sample, as shown in Fig. 4.

We calculated two types of the Purcell factor. One is called the full Purcell factor ( $\text{FP}_F$ ) which shows the total enhancement of the radiated power of the dipole. It can be found through the real part of the input impedance of the lossless Hertzian dipole which is equal to its radiation resistance. Keeping the same current in the dipole in the presence of the metamaterial sample and in its absence the ratio of radiation resistances delivers the gain in the radiated power  $\text{FP}_F$ . The second type of the Purcell factor is called the radiative Purcell factor ( $\text{RP}_F$ ). It determines the enhancement of the power radiated by the

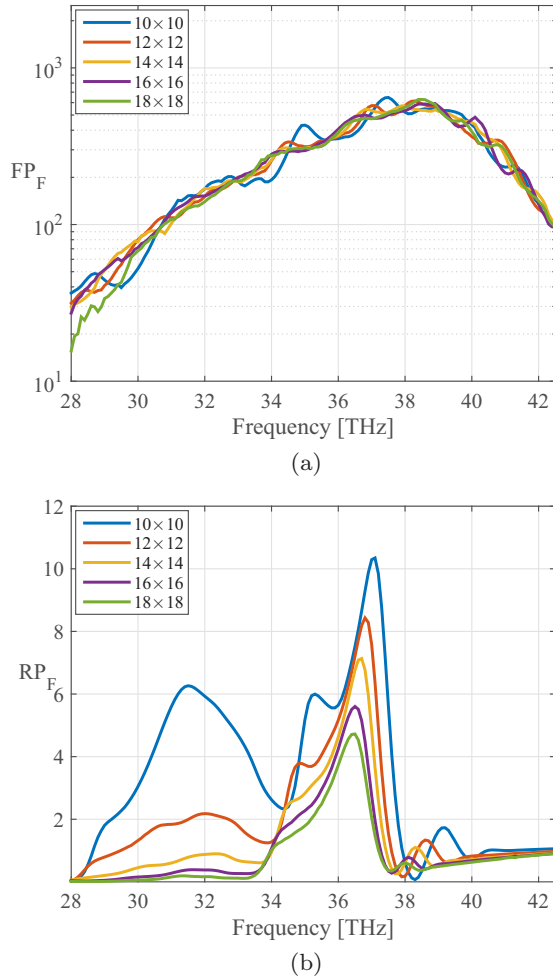


FIG. 5. (Color online) The Purcell factor for different sizes of the cubic metamaterial blocks comprised of the lithium tantalate wire medium. These sizes correspond to  $10 \times 10$ ,  $12 \times 12$ ,  $14 \times 14$ ,  $16 \times 16$ , and  $18 \times 18$  nanowires, respectively. To maintain a cubic shape for the material, different sample cylinder lengths are considered in each case. A full-wave 3D simulation has been employed. (a) Full Purcell factor. (b) Radiative Purcell factor. Here,  $a = 32$  and  $b = 200$  nm.

same dipole moment into free space.  $RP_F$  is calculated via the power flux integrated in the far zone in the presence of the sample and in its absence. Indeed, initially, the Purcell effect [31,32] was treated as an increase of the spontaneous decay rate of an emitter located in a resonant cavity.

An important check of the reliability of our simulations was done by setting the optical losses in lithium tantalate to zero. Then the absorption of radiated power in the sample, i.e., the nonradiative part of the full Purcell factor, vanishes and  $FP_F = RP_F$ .

### A. Longitudinal dipole emitter

The geometry and orientation of the dipole are shown in Fig. 4.

Figure 5(a) depicts the full Purcell factor versus frequency. To be sure that our effect is not distorted by dimensional resonances, we simulated the cubic-shape sample with five sizes of the edge, corresponding to  $10 \times 10$ ,  $12 \times 12$ ,  $14 \times 14$ ,

$16 \times 16$ , and  $18 \times 18$  nanowires, respectively (the internal structure of the wire medium was kept the same, which means the length of nanowires varying from 1.8 to 3.4 microns). As it is seen, the dimensional resonances do not enter the selected frequency range, i.e., the full Purcell factor in all cases emulates the infinite wire medium. About the frequency  $f = 38$  THz, the full Purcell factor has its maximum value, whereas the homogenization model predicts the maximum at  $f = 39$  THz. This small error is not surprising. First, the nonlocal homogenization model, though the most accurate of the known effective-medium models of wire media, is still an analytical approximation. Second, the whole theory of Sec. II neglects optical losses, though they are quite substantial. Notice that these high losses make the resonance of the Purcell factor in Fig. 5(a) not very pronounced. Indeed, in a lossy medium, the topological transition cannot be sharp. It happens not at a single frequency, but across a certain frequency interval. Another reason why the resonance in Fig. 5(a) is not sufficiently pronounced is the logarithmic scale of the plot.

Whereas the full Purcell factor can exceed 600 at the transition frequency, the radiative Purcell factor shown in Fig. 5(b) is not very high. However, it is still remarkable at the resonance. The global maximum was achieved for the sample of  $10 \times 10$  nanowires, and the maximum occurs at nearly  $f = 37$  THz. If the size of the sample is smaller, the sample becomes mesoscopic (the full Purcell factor starts to feel the sample size) and, on the other hand, if the size of the sample is larger, the maximum of the radiative Purcell factor decreases monotonously versus the size, which means that the internal reflections have no visible impact. At the resonant frequency, the reflection at the interface with free space is not significant because the wave impedance of the sample is relatively matched to the free-space wave impedance. This matching allows the electromagnetic wave to exit from the sample. The smallness of the radiative Purcell factor compared to the full one can result from the attenuation of the radiation in the sample.

As to other frequencies, around the topological phase transition range, the internal reflections become important due to the wave impedance mismatch. Close to the resonant frequency, the radiative Purcell factor drops dramatically because the metamaterial sample experiences the strong wave impedance mismatching at the interface. This mismatch definitely implies standing waves; however, the dimensional resonances do not arise due to the high attenuation. At low frequencies where the open-surface regime only exists, a local maximum is seen that is most visible for the sample of  $10 \times 10$  nanowires. This local maximum at  $f = 32$  THz is also due to the impedance matching since it exists for all sizes of the sample.

Figures 6(a) and 6(b) compare the full Purcell factor and radiative Purcell factor, respectively, for several radii of nanowires while the lattice constant is fixed. According to Eq. (8), by changing the radius, i.e., the volume fraction, we change  $\epsilon_r$  and, consequently, shift the frequency of the topological transition. This frequency shift is clearly seen in the figures for both full and radiative Purcell factors.

### B. Perpendicular dipole emitter

In this section, we report the results of similar calculations for the perpendicular dipole (with the same absolute value of the dipole moment as above) and compare to the previous ones

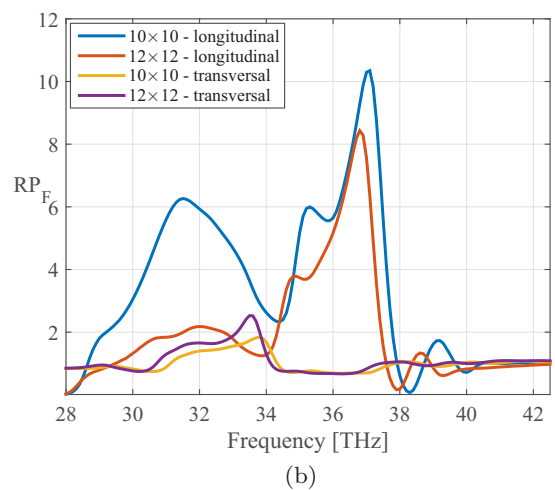
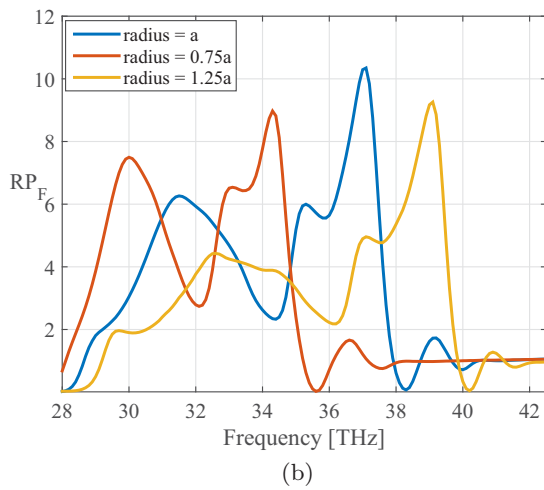
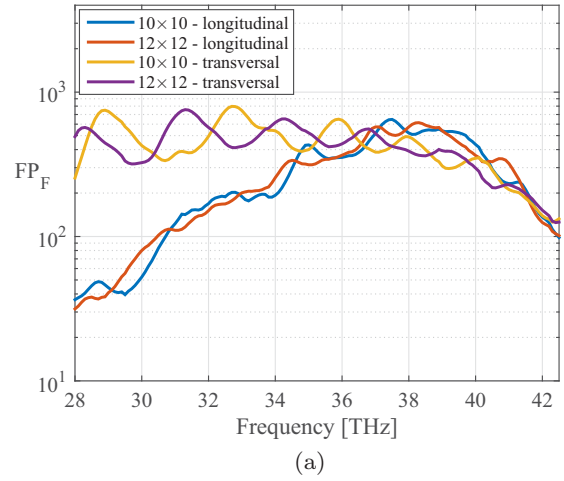
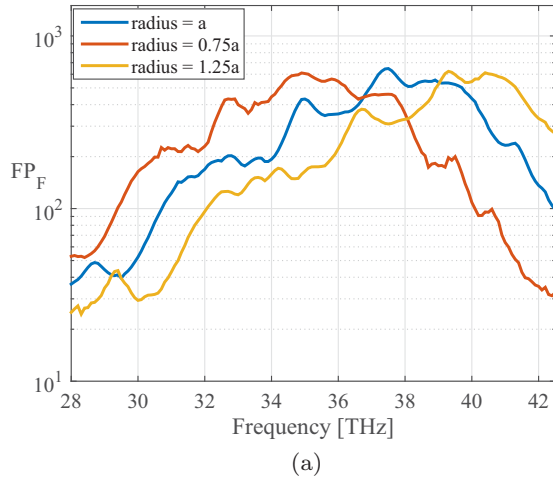


FIG. 6. (Color online) The Purcell factor for different radii of wires in a lithium tantalate cubic-shape wire medium including  $10 \times 10$  nanowires. (a) Full Purcell factor. (b) Radiative Purcell factor. Here,  $a = 32$  and  $b = 200$  nm.

FIG. 7. (Color online) The Purcell factor for two different orientations of the dipole. Two samples of a lithium tantalate cubic-shape wire medium including  $10 \times 10$  and  $12 \times 12$  nanowires are considered. (a) Full Purcell factor. (b) Radiative Purcell factor. Here,  $a = 32$  and  $b = 200$  nm.

obtained for a parallel one. For better clarity of our plots, we show the results only for two cubic-shape samples:  $10 \times 10$  and  $12 \times 12$  nanowires.

Figure 7(a) shows that the perpendicular dipole does not feel the topological transition. Definitely, the radiation decreases above  $f = 40$  THz, where the dispersion surface is closed. However, at the frequency range where the topological transition happens for the parallel dipole, the Purcell factor for the perpendicular one is the same as below—in the “standard” open-surface regime. This fully agrees with our theoretical expectations. The Purcell factor of the perpendicular dipole turns out to be smaller than that of the parallel dipole (this result keeps the same for other sizes of the sample) at the transition. In particular, the insensitivity of the perpendicular dipole to the topological transition is seen in the plot for the radiative Purcell factor, depicted in Fig. 7(b). The longitudinal (parallel) dipole is much more efficient for radiation to free space than the perpendicular one. For it, the radiative Purcell factor does not exceed 2 and equals unity in the range of the topological transition and around. This is definitely the result of the strong wave impedance mismatch. Since the medium is anisotropic,

the regime  $\epsilon_{\parallel} \approx 0$  mimics the  $\epsilon$ -near-zero regime only for the radiation of the parallel dipole (with dominating parallel polarization), whereas the radiation of the perpendicular dipole almost does not feel the zero of  $\epsilon_{\parallel}$  and turns out to be confined inside the sample. Therefore, the contrast between  $RP_F$  of the parallel and perpendicular dipoles at about the transition frequency is tenfold for the sample including  $10 \times 10$  nanowires.

#### IV. CONCLUSIONS

In this work, we have theoretically revealed and studied a topological phase transition in a wire medium which may occur in the frequency range where the homogenization model is still valid. We utilized the spatial dispersion inherent to a wire medium in order to engineer the unbounded spatial spectrum of propagating eigenmodes at the transition frequency. The open and closed parts of the dispersion surface in this regime touch each other at a special point in the reciprocal space of the lattice. At this point, the real part of the parallel component of the effective permittivity is zero. We found the practical

design parameters for lithium tantalate nanowires which allow one to implement this regime. Due to this effect (topological phase transition over the wave-vector axis at one certain frequency), we obtained by exact numerical simulations a dramatic increase of the radiated power of a subwavelength electric dipole located at the center of the finite-size sample of our wire medium. The highest Purcell factor corresponds to the parallel oriented dipole, which represents the contrast to previously known results where the high Purcell factors of wire media were reported only for the perpendicular dipoles. Whereas the radiation of the parallel dipole is resonant with the maximum at the transition frequency, the radiation of the

perpendicular dipole is rather stable in the frequency range of open-surface dispersion and smoothly decreases at higher frequencies where the dispersion surface becomes closed. We also investigated the radiative Purcell factor. It attains one order of magnitude for a parallel dipole. Finally, since lithium tantalate is a lossy material, and the radiative Purcell factor we have reported is modest, we plan to reveal the same regime for a wire medium of SiC or GaN, where  $RP_F$  may approach more closely to the resonant value of the full Purcell factor, e.g., attain two orders of magnitude. Then we will organize an experimental verification of our effect.

- 
- [1] V. G. Veselago, The electrodynamics of substances with simultaneously negative values of  $\epsilon$  and  $\mu$ , *Sov. Phys. Usp.* **10**, 509 (1968).
- [2] U. Leonhardt, Optical conformal mapping, *Science* **312**, 1777 (2006).
- [3] J. B. Pendry, Negative Refraction Makes a Perfect Lens, *Phys. Rev. Lett.* **85**, 3966 (2000).
- [4] Y. Liu, G. Bartal, and X. Zhang, All-angle negative refraction and imaging in a bulk medium made of metallic nanowires in the visible region, *Opt. Express* **16**, 15439 (2008).
- [5] M. S. Mirmoosa and C. R. Simovski, Micron-gap thermophotovoltaic systems enhanced by nanowires, *Photon. Nanostruct. Fundam. Appl.* **13**, 20 (2015).
- [6] S. Molesky, C. J. Dewalt, and Z. Jacob, High temperature epsilon-near-zero and epsilon-near-pole metamaterial emitters for thermophotovoltaics, *Opt. Express* **21**, A96 (2013).
- [7] L. Novotny and B. Hecht, *Principles of Nano-Optics* (Cambridge University Press, Cambridge, UK, 2006).
- [8] A. Poddubny, I. Irosh, P. Belov, and Y. Kivshar, Hyperbolic metamaterials, *Nat. Photon.* **7**, 948 (2013).
- [9] Z. Jacob, I. I. Smolyaninov, and E. E. Narimanov, Broadband Purcell effect: Radiative decay engineering with metamaterials, *Appl. Phys. Lett.* **100**, 181105 (2012).
- [10] A. N. Poddubny, P. A. Belov, and Y. S. Kivshar, Spontaneous radiation of a finite-size dipole emitter in hyperbolic media, *Phys. Rev. A* **84**, 023807 (2011).
- [11] D. R. Smith and D. Schurig, Electromagnetic Wave Propagation in Media with Indefinite Permittivity and Permeability Tensors, *Phys. Rev. Lett.* **90**, 077405 (2003).
- [12] C. R. Simovski, P. A. Belov, A. V. Atrashchenko, and Y. S. Kivshar, Wire metamaterials: Physics and applications, *Adv. Mater.* **24**, 4229 (2012).
- [13] A. V. Chebykin, A. A. Orlov, C. R. Simovski, Yu. S. Kivshar, and P. A. Belov, Nonlocal effective parameters of multilayered metal-dielectric metamaterials, *Phys. Rev. B* **86**, 115420 (2012).
- [14] M. G. Silveirinha, Nonlocal homogenization model for a periodic array of  $\epsilon$ -negative rods, *Phys. Rev. E* **73**, 046612 (2006).
- [15] I. M. Lifshitz, Anomalies of electron characteristics of a metal in the high pressure region, *Sov. Phys. JETP* **11**, 1130 (1960).
- [16] H. N. S. Krishnamoorthy, Z. Jacob, E. Narimanov, I. Kretzschmar, and V. M. Menon, Topological transitions in metamaterials, *Science* **336**, 205 (2012).
- [17] D. W. Prather, S. Shi, A. Sharkawy, J. Murakowski, and G. Schneider, *Photonic Crystals, Theory, Applications and Fabrication* (Wiley, Hoboken, NJ, 2009).
- [18] S. Foteinopoulou, M. Kafesaki, E. N. Economou, and C. M. Soukoulis, Two-dimensional polaritonic photonic crystals as terahertz uniaxial metamaterials, *Phys. Rev. B* **84**, 035128 (2011).
- [19] M. A. Gorlach and P. A. Belov, Effect of spatial dispersion on the topological transition in metamaterials, *Phys. Rev. B* **90**, 115136 (2014).
- [20] X. Yang, C. Hu, H. Deng, D. Rosenmann, D. A. Czaplewski, and J. Gao, Experimental demonstration of near-infrared epsilon-near-zero multilayer metamaterial slabs, *Opt. Express* **21**, 23631 (2013).
- [21] E. Reyes-Gomez, S. B. Cavalcanti, L. E. Oliveira, and C. A. A. de Carvalho, Metric-signature topological transitions in dispersive metamaterials, *Phys. Rev. E* **89**, 033202 (2014).
- [22] A. N. Poddubny, P. A. Belov, and Y. S. Kivshar, Purcell effect in wire metamaterials, *Phys. Rev. B* **87**, 035136 (2013).
- [23] V. V. Vorobev and A. V. Tyukhtin, Nondivergent Cherenkov Radiation in a Wire Metamaterial, *Phys. Rev. Lett.* **108**, 184801 (2012).
- [24] L. B. Felsen and N. Marcuvitz, *Radiation and Scattering of Waves* (IEEE, New York, 1994).
- [25] E. E. Narimanov, Photonic Hypercrystals, *Phys. Rev. X* **4**, 041014 (2014).
- [26] P. Shekhar, J. Atkinson, and Z. Jacob, Hyperbolic metamaterials: Fundamentals and applications, *Nano Converg.* **1**, 14 (2014).
- [27] Mahi R. Singh, Polaritonics in nanowires made from dispersive materials, *Phys. Rev. B* **80**, 195303 (2009).
- [28] C. Kittel, *Introduction to Solid State Physics* (Wiley, New York, 1976).
- [29] M. Schall, H. Helm, and S. R. Keiding, Far infrared properties of electro-optic crystals measured by THz time-domain spectroscopy, *Int. J. Infrared Millim. Waves* **20**, 595 (1999).
- [30] T. F. Crimmins, N. S. Stoyanov, and K. A. Nelson, Heterodyned impulsive stimulated Raman scattering of phonon-polaritons in LiTaO<sub>3</sub> and LiNbO<sub>3</sub>, *J. Chem. Phys.* **117**, 2882 (2002).
- [31] E. M. Purcell, Spontaneous emission probabilities at radio frequencies, *Phys. Rev.* **69**, 674 (1946).
- [32] C. Sauvan, J. P. Hugonin, I. S. Maksymov, and P. Lalanne, Theory of the Spontaneous Optical Emission of Nanosize Photonic and Plasmon Resonators, *Phys. Rev. Lett.* **110**, 237401 (2013).